Spatial interpolation of precipitation in a dense gauge network for monsoon storm events in the southwestern United States

Matthew Garcia,[1,2] Christa D. Peters-Lidard,[2] and David C. Goodrich[3]

Received 30 November 2006; revised 15 August 2007; accepted 11 September 2007; published 15 March 2008.

[1] Inaccuracy in spatially distributed precipitation fields can contribute significantly to the uncertainty of hydrological states and fluxes estimated from land surface models. This paper examines the results of selected interpolation methods for both convective and mixed/stratiform events that occurred during the North American monsoon season over a dense gauge network at the U.S. Department of Agriculture Agricultural Research Service Walnut Gulch Experimental Watershed in the southwestern United States. The spatial coefficient of variation for the precipitation field is employed as an indicator of event morphology, and a gauge clustering factor *CF* is formulated as a new, scale-independent measure of network organization. We consider that $CF < 0$ (a more distributed gauge network) will produce interpolation errors by reduced resolution of the precipitation field and that $CF > 0$ (clustering in the gauge network) will produce errors because of reduced areal representation of the precipitation field. Spatial interpolation is performed using both inverse-distance-weighted (IDW) and multiquadric-biharmonic (MQB) methods. We employ ensembles of randomly selected network subsets for the statistical evaluation of interpolation errors in comparison with the observed precipitation. The magnitude of interpolation errors and differences in accuracy between interpolation methods depend on both the density and the geometrical organization of the gauge network. Generally, MQB methods outperform IDW methods in terms of interpolation accuracy under all conditions, but it is found that the order of the IDW method is important to the results and may, under some conditions, be just as accurate as the MQB method. In almost all results it is demonstrated that the inverse-distance-squared method for spatial interpolation, commonly employed in operational analyses and for engineering assessments, is inferior to the ID-cubed method, which is also more computationally efficient than the MQB method in studies of large networks.

Citation: Garcia, M., C. D. Peters-Lidard, and D. C. Goodrich (2008), Spatial interpolation of precipitation in a dense gauge network for monsoon storm events in the southwestern United States, *Water Resour. Res.*, *44*, W05S13, doi:10.1029/2006WR005788.

1. Introduction

[2] Land surface models (LSMs) of hydrological processes rely principally on accurate observations of precipitation for the simulation of soil moisture states, land-atmosphere fluxes, and surface runoff for stream discharge estimation, numerical weather prediction and water resources applications over a wide range of spatial and temporal scales [e.g., *Woods and Sivapalan*, 1999; *Cosgrove et al.*, 2003; *Carpenter and Georgakakos*, 2004]. The spatially distributed application of an LSM over a region of interest requires the application of similarly distributed precipitation fields that can be derived from various sources, including surface gauge networks, surface-based radar, and orbital platforms. The spatial variability of precipitation influences the spatial organization of soil temperature and moisture states and, consequently, the spatial variability of land-atmosphere fluxes [e.g., *Taylor et al.*, 1997; *Nykanen et al.*, 2001]. The accuracy of spatially distributed precipitation fields can contribute significantly to the uncertainty of model-based hydrological states and fluxes at the land surface, as found by *Faurès et al.* [1995], *Chaubey et al.* [1999], *Nijssen and Lettenmaier* [2004], and others.

[3] We address the application of spatial interpolation methods to observations of precipitation events during the North American monsoon (NAM) [*Adams and Comrie*, 1997; *Higgins et al.*, 1997] using a dense surface precipitation gauge network operated by the U.S. Department of Agriculture (USDA) Agricultural Research Service (ARS) in the southwestern United States [*Goodrich et al.*, 2008]. The position examined here is that an interpolated precipitation field retains a degree of resemblance to the actual or true precipitation field that depends on both the geometry of the observing network and on the mathematics of the interpolation method. The observing network can be described primarily by its configuration in space, its regularity of network organization, a characteristic spatial scale of representation, physiographic and climatological biases, etc.

[1] Goddard Earth Science and Technology Center, University of Maryland Baltimore County, Baltimore, Maryland, USA.
[2] Hydrological Sciences Branch, NASA Goddard Space Flight Center, Greenbelt, Maryland, USA.
[3] Southwest Watershed Research Center, Agricultural Research Service, U.S. Department of Agriculture, Tucson, Arizona, USA.

Issues of spatial scale [*Eagleson*, 1967], geometric regularity [*Smith et al.*, 1986], and representative bias [*Briggs and Cogley*, 1996] in gauge network configuration have been examined previously in the literature and are mentioned here only as background in the further examination of network organization and the interpolation methods themselves.

[4] This work differs significantly from previous efforts at the description of gauge network configuration methods [*Rodríguez-Iturbe and Mejía*, 1974; *Bras and Rodríguez-Iturbe*, 1976; *Pardo-Igúzquiza*, 1998; *Bradley et al.*, 2002] and of simple comparisons of interpolation results for existing networks [*Franke*, 1982; *Ball and Luk*, 1998; *Syed et al.*, 2003]. The subjectivity of geostatistical (kriging) methods lends significant uncertainty to their results and those methods are not easily configured for automatic or operational applications. This work thus evaluates the applicability of two objective interpolation methods under contrasting precipitation event morphologies. We seek to address the following issues: (1) statistical distinctions within and between events of different convective morphology for simplistic and sophisticated objective interpolators, (2) the possible impact of gauge network configuration on the performance of these interpolators, and (3) selection of objective interpolators that account for both network geometry and event morphology.

[5] Convective precipitation variability, with a characteristic spatial scale on the order of 1 km [*Blöschl and Sivapalan*, 1995; *Skøien et al.*, 2003], is difficult to diagnose with sparse surface gauge networks and even with surface-based radar observations. *Germann and Joss* [2001] employed variogram analyses for the examination of precipitation spatial continuity during the Mesoscale Alpine Programme and found that spatial variation was well correlated with convective activity. The potential importance of the relative spatial variance as an indicator of network accuracy was identified by *Tsintikidis et al.* [2002]. This work seeks to extend that consideration of spatial variance from the observing network to the morphology of the precipitation event itself. Our methodology depends on the application of a number of network gauges to the determination of precipitation at a greater number of desired locations than the network can provide, such as the interpolation of a sparse gauge network to a high-resolution grid. One might contrast this problem with the opposite task of finding the appropriate averaged precipitation for a coarse resolution grid cell from the observations of many gauges covered there [e.g., *Rodríguez-Iturbe and Mejía*, 1974; *McCollum and Krajewski*, 1998].

[6] Two methods of spatial interpolation are examined here. The first is an inverse-distance-weighted approach that can be found in numerous references oriented at the practical application of precipitation observations to forecasting and engineering problems. The second is the multiquadric-biharmonic method reviewed by *Hardy* [1990], a more holistic (regarding area of influence) but computationally intensive method of interpolation that can be applied objectively and has been compared favorably with geostatistical methods [e.g., *Supachai*, 1988; *Syed et al.*, 2003]. The sensitivity analyses described here evaluate these two spatial interpolation methods for their ability, using subsets of the given gauge network, to reproduce by interpolation the precipitation field found with observations over the complete network.

[7] This paper is organized as follows: the study location and data sources are described in section 2 with a brief description of the method of event characterization supporting the selection of precipitation events for this study. A brief comment on potential orographic influences on the observed precipitation is provided there. Measures of precipitation gauge network organization and geometry, spatial interpolation methods and error metrics examined, and a description of the methods employed in this work are contained in section 3. Results are discussed in section 4, and conclusions and potential applications are presented in section 5.

2. Study Location and Selected Events

[8] The Walnut Gulch Experimental Watershed (WGEW) is located southeast of Tucson, Arizona, in a semiarid region of Arizona and is operated and maintained by the USDA Agricultural Research Service (ARS), Southwest Watershed Research Center (SWRC). Nearly 100 precipitation and runoff gages are operated on a continuous basis within the watershed area of approximately 150 km^2 [*Goodrich et al.*, 1997]. The SWRC currently provides breakpoint [*Sansom*, 1992] and summary records of precipitation events in the WGEW in an online archive [*Goodrich et al.*, 2008]. During its period of operation, the WGEW has served as a study site for several field experiments including Monsoon'90 [*Kustas et al.*, 1991], the Soil Moisture Experiments in 2004 (SMEX04) [*Jackson and Lettenmaier*, 2004], and the international North American Monsoon Experiment (NAME) [*Higgins et al.*, 2006]. The WGEW hosts a soil profile instrumentation site within the USDA Natural Resources Conservation Service (NRCS) Soil Climate Analysis Network (SCAN, http://www.wcc.nrcs.usda.gov/scan) in addition to a variety of other hydrometeorological and watershed observation sites.

[9] The locations of precipitation gauges within the WGEW are shown by *Goodrich et al.* [2008, Figure 2] and here in Figure 1. Given that network, 85 gauges were selected from an archive set of 95 locations on the basis of record continuity throughout the study period. Considering only the 85 gauge locations employed in this study, the WGEW contains one of the most dense precipitation gauge networks in the world ($\sim$0.570 gauges km^{-2}).

[10] The two events studied here were identified from the largest occurrences of daily total precipitation, indicated by WGEW network mean values, in August of each year during 1990–2003. The daily variability of August precipitation at the WGEW is illustrated in Figure 2, where the value plotted for each day is the mean precipitation amount during the study period, and the bottom of the corresponding error bar represents the median total precipitation for that day. The top of an error bar in Figure 2 denotes the quantity of precipitation that is one standard deviation above the mean for that day, giving some indication of the large variance in August daily precipitation that can be expected. Dates with the largest daily total precipitation in each August are listed in Table 1 and serve as our study sample.

[11] The climatological daily precipitation in August shown in Figure 2 is generally consistent with the onset phase of the NAM system in the southwestern United States and the occurrence of air mass thunderstorms fed by monsoonal moisture sources [*Simanton and Osborn*, 1980; *Adams and Comrie*, 1997; *Higgins et al.*, 1997]. The events

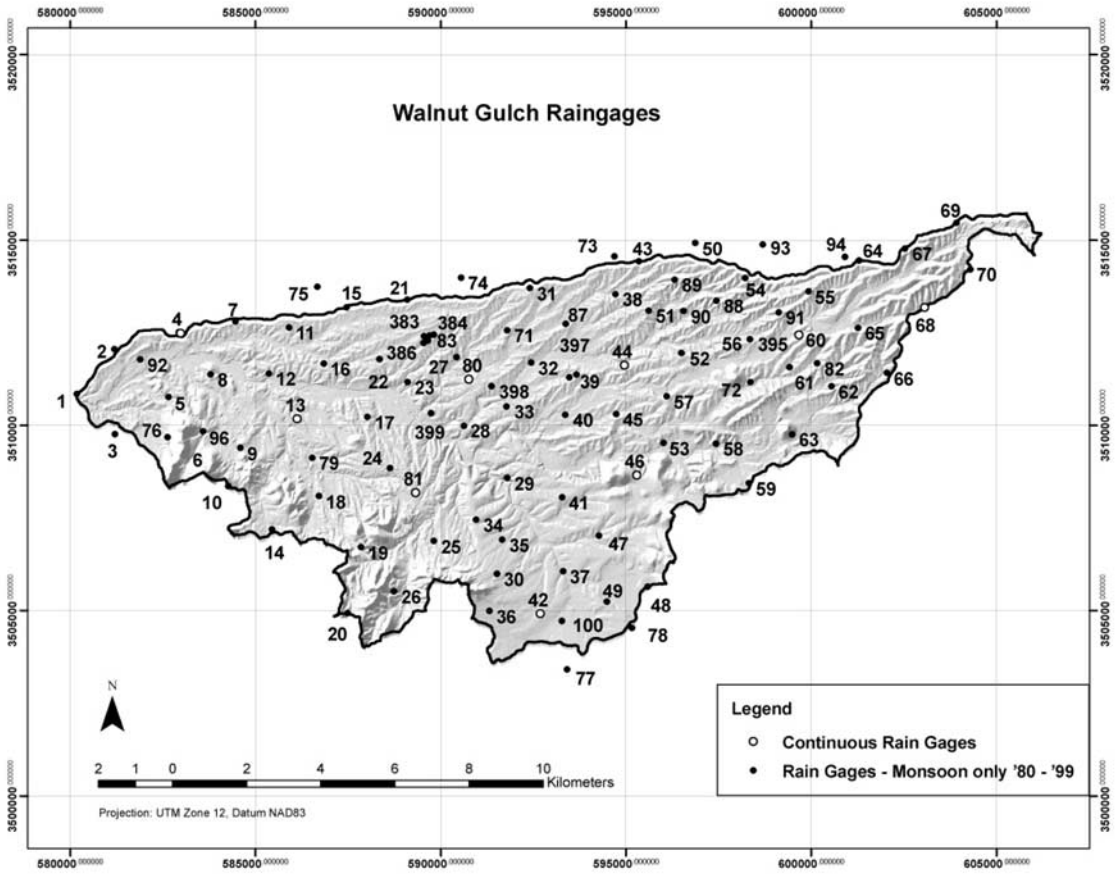

Figure 1. Precipitation gauge network at the USDA-ARS Walnut Gulch Experimental Watershed (WGEW) [after *Goodrich et al.*, 2008]. Location references are given in UTM coordinates (meters) for zone 12.

listed in Table 1 demonstrate considerable ambiguity with respect to orographic influence: some events, such as the two examined in detail below, actually have a negative correlation of total precipitation with gauge elevation, while others show neutral (zero) and small positive correlations. It should be considered that the WGEW is not necessarily of sufficient size for demonstration of orographic influences on the mesoscale meteorology, and any further examination of

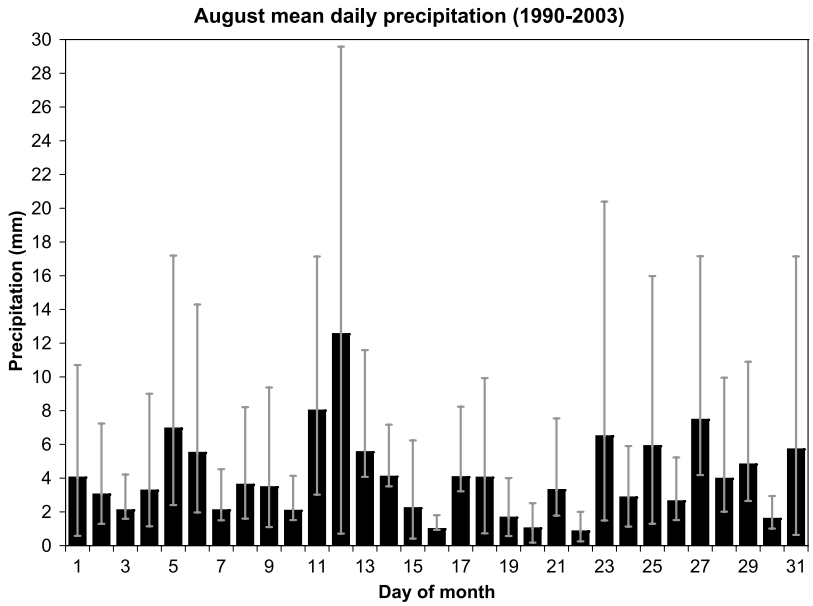

Figure 2. Precipitation in August for the considered period (1990–2003), shown as daily totals averaged over all years in the study period and all stations in the WGEW gauge network.

Table 1. Dates and Statistics of the Largest August Precipitation Events for 1990–2003 at the USDA-ARS WGEW

	WGEW Observed Precipitation Statistics				
Date	Minimum, mm	Maximum, mm	Mean, mm	Variance, mm^2	Spatial CV
12 Aug 1990	**21.6**	**83.1**	**39.3**	**164.8**	**0.327**
9 Aug 1991	0.0	29.0	16.6	32.4	0.344
23 Aug 1992	27.9	55.1	40.8	29.3	0.133
31 Aug 1993	15.2	80.0	35.4	155.3	0.352
25 Aug 1994	10.4	59.7	27.8	113.2	0.382
18 Aug 1995	0.8	57.7	16.3	110.6	0.646
18 Aug 1996	**0.0**	**67.9**	**13.2**	**310.9**	**1.336**
5 Aug 1997	18.3	92.9	39.3	256.6	0.408
12 Aug 1998	5.3	70.1	33.4	297.2	0.516
5 Aug 1999	9.9	43.2	21.6	66.8	0.379
6 Aug 2000	4.8	63.2	25.8	234.4	0.593
29 Aug 2001	11.2	39.4	21.5	54.5	0.343
1 Aug 2002	4.8	39.9	16.1	65.9	0.506
27 Aug 2003	1.1	73.4	31.0	285.0	0.545

topographic and meteorological patterns on a scale larger than the WGEW remains beyond the scope of this work. For these reasons, orographic influences and the surface topography are excluded from the application of interpolation methods described below.

[12] We utilize the spatial coefficient of variation (*CV*) of the precipitation field, calculated as the ratio of the standard deviation to the arithmetic mean intensity of the observed daily total precipitation across the study area, as an indicator of convective character. Accordingly, we selected two events with low and high spatial *CV* for detailed study, as shown in bold type in Table 1. The selection of an event in 1990 contributes to collaborative research on Monsoon'90 experimental observations and resulting soil moisture and surface flux patterns in the WGEW. For comparison and contrast, the largest event in August 1996 was also selected for its significantly larger value of spatial *CV*, despite its smaller mean and maximum precipitation intensity.

[13] This work follows in part on the efforts of *Germann and Joss* [2000, 2001] toward the correlation of spatial variation in precipitation intensity with event morphology. We employ a method that is considerably less complex than the radar reflectivity variogram analysis in that work with our calculation of the spatial *CV*. However, it remains difficult to judge the threshold at which one event appears convective and another appears more stratiform solely on the basis of the calculation of spatial *CV*. In light of previous studies [e.g., *Steiner and Smith*, 1998], we considered the spectrum of events listed in Table 1 and the likely convective characteristics associated with each on the basis of both the time series of precipitation (as aggregated hourly totals) during the event and its spatial *CV*. Overall, we expect purely convective-based precipitation fields to exhibit greater spatial variance (*CV*) because of the concentration of convective cells. Smaller spatial variation (*CV*) would be found for purely stratiform events because of the relative uniformity of precipitation over the study region. With these considerations, we have specified an arbitrary threshold around $CV = 0.5$, above which the event is considered convective, and below which the event may demonstrate mixed convective-stratiform or primarily stratiform periods of precipitation. As shown in Table 1, one event from each range is identified for analysis here.

2.1. Event 1: 12 August 1990

[14] The first event selected included the largest daily total precipitation in the WGEW around the time of the Monsoon'90 field experiment on 12 August 1990. The spatial distribution of total precipitation during this event is shown in Figure 3, as derived using the inverse-distance-cubed interpolation method described below. During this event, the network mean precipitation over the area of the WGEW was 39.3 mm, with maximum totals greater than 70 mm and minimum totals less than 25 mm. As listed in Table 1, a value of $CV = 0.327$ was observed for this event that occurred primarily over a 7-h period beginning in the early morning (~0200 MST) on 12 August 1990.

[15] On the basis of analyzed hourly precipitation totals, the first 2 h of the storm were dominated by large precipitation rates, in some locations exceeding 40 mm h^{-1} and indicative of leading convection in a squall line system. Within the first hour of the event, only a portion of the WGEW was affected by the passing convective line and spatial $CV > 1.6$ was observed. For the 2 h with intense convection, network mean total precipitation for this period of the storm event was approximately 25 mm with spatial

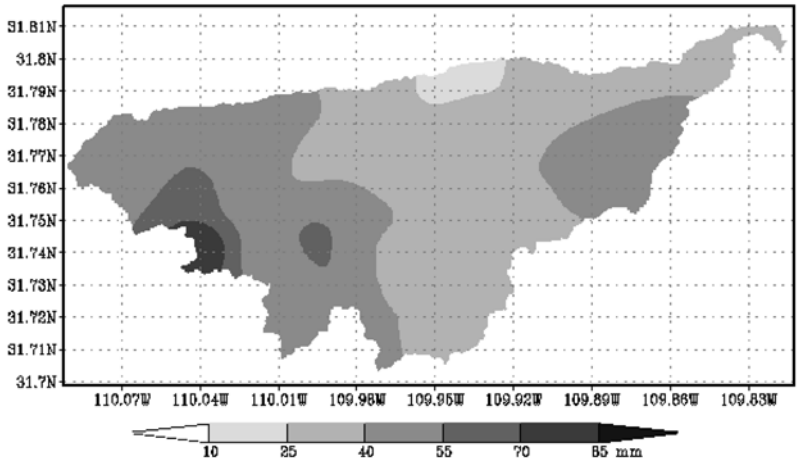

Figure 3. Event 1 (12 August 1990) total precipitation (mm) over the WGEW area, as derived using the inverse-distance-cubed interpolation method described in the text.

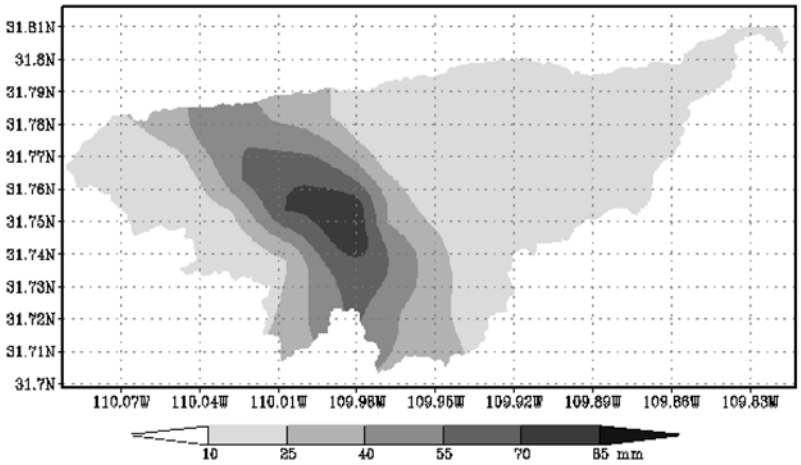

Figure 4. Event 2 (18 August 1996) total precipitation (mm) over the WGEW area, as derived using the inverse-distance-cubed interpolation method described in the text.

CV = 0.517. For the later portion of the storm event, with precipitation rates generally less than 10 mm h^{-1}, the network mean total precipitation was approximately 15 mm with overall spatial CV = 0.402.

[16] With the observation of these two CV regimes in a single event, we must consider the occurrence of propagating storms that can produce heavy precipitation in some areas but overall more moderate total (network mean) precipitation over the duration of the event and thus moderate values of spatial CV. The observed configuration of leading convection and trailing stratiform regions follows the conceptual archetype for midlatitude squall lines [e.g., *Parker and Johnson*, 2000, 2004; *Houze*, 2004]. During the storm event, spatial CV may thus shift from large to small values according to the passage of the convective, and then stratiform, precipitation structures within such a squall-like event. Overall, spatial CV may finally obtain a moderate or low value when the storm event total precipitation is analyzed because of both the translation of the leading convective line and the temporal dominance and overall smoothing effects on the total precipitation field provided by the trailing stratiform portion of the storm event.

2.2. Event 2: 18 August 1996

[17] The second event selected, on 18 August 1996, was chosen because of its spatial concentration and overall intensity within a short storm period. The spatial distribution of total precipitation during this event is shown in Figure 4, also using the inverse-distance-cubed interpolation method as described below. During this event, the network mean precipitation over the area of the WGEW was only 13.2 mm, but had maximum totals greater than 60 mm and minimum totals of 0.0 mm. The spatial CV = 1.336 for this event as listed in Table 1.

[18] This event occurred over approximately 2 h in the afternoon (~1500 MST) on 18 August 1996 and demonstrated the localized characteristics of an air mass thunderstorm event [e.g., *Raymond*, 1981; *Faurès et al.*, 1995]. Radiosonde-based profiles of temperature, humidity and winds at Tucson, Arizona, around the time of this event (provided by the University of Wyoming, Department of Atmospheric Science) are generally consistent with the type III pattern for severe thunderstorm events over central Arizona that was found by *Maddox et al.* [1995].

3. Network Configuration Analyses and Spatial Interpolation Methods

[19] In determining the characteristics of precipitation field samples by common methods of observation, we must consider the limitations of both the equipment and its deployment. Individual precipitation gauges in a network are subject to errors in mechanical operation and intensity-dependent calibration [*Humphrey et al.*, 1997], site considerations such as sheltering [*Upton and Rahimi*, 2003], and wind-related effects [*Larson and Peck*, 1974; *Sevruk*, 1996].

[20] The configuration geometry of gauge networks has been explored consistently over the past several decades for various purposes, e.g., research, management and economic objectives [*Rodríguez-Iturbe and Mejía*, 1974; *Bras and Rodríguez-Iturbe*, 1976; *Pardo-Igúzquiza*, 1998]. The regional collection of data is oriented ideally on the minimization of estimation error, instrumentation cost, and scientific analysis. Regional regression analyses of network observations, such as stream gauge data sets [*Matalas and Gilroy*, 1968], allow for the evaluation of gauge site "performance" in a network as well as for field estimation at ungauged sites. *Rodríguez-Iturbe and Mejía* [1974] and later researchers thus often focused on network design for regional and long-term mean estimates of precipitation, with specific attention to spatial and temporal correlation of observations, the available number of stations, and the optimum network geometry [*Bradley et al.*, 2002].

3.1. Gauge Network Configuration

[21] The density of a given network is given simply by

$$D = \frac{N}{A}, \tag{1}$$

where N is the number of gauge locations in the complete network, or a selected subset, and A is the area of the study region. However, considering only the network density ignores the geometrical configuration of gauges in the network, prompting statistical evaluations of the network by

ensemble experiments [e.g., *Bradley et al.*, 2002]. *Morrissey et al.* [1995] had previously concluded that the standard error of observations in a network depends on that geometrical configuration, and not just on the density of stations and the spatial structure of the measured field. It may thus be considered that an imposed or generalized spatial structure for an observed field such as precipitation, as results from a geostatistical approach, could be inappropriate. Overall, Morrissey et al. concluded that uniform networks are best in the spectrum of observation accuracy, followed by random, quasi-linear, and finally clustered networks.

[22] The intergauge distance is found by location-based calculations for all gauge-to-gauge combinations in a given network, and the mean and variance (or standard deviation) of this distribution are important here. Also calculated is the unbiased coefficient of skewness for the distribution of intergauge distances,

$$\gamma_d = \frac{N}{(N-1)(N-2)} \sum_{n,m=1}^{N} \left(\frac{d_{n,m} - \mu_d}{\sigma_d} \right)^3, \qquad (2)$$

where $\{n, m\}$ are gauge indices, $d_{n,m}$ is the distance between the two gauge locations, and μ_d and σ_d are the mean and standard deviation for the distribution of intergauge distances, respectively.

[23] We consider also the distribution of nearest-neighbor distance and its moments for a given gauge network. *Smith et al.* [1986] considered the mean of that distribution, but we are particularly interested in its coefficient of skewness. We suggest that this constitutes a clustering factor (*CF*) for the network, found with an unbiased formulation analogous to equation (2) as

$$CF = \gamma_{nn} = \frac{N}{(N-1)(N-2)} \sum_{n=1}^{N} \left(\frac{d_{nn} - \mu_{nn}}{\sigma_{nn}} \right)^3, \qquad (3)$$

where n is a gauge index, d_{nn} is the distance to its nearest neighboring gauge, and μ_{nn} and σ_{nn} are the mean and standard deviation for the distribution of nearest-neighbor distances, respectively.

[24] Examples of these measures are illustrated in Figures 5 and 6, where the geometric statistics for four different gauge network configurations are calculated. Figure 5a shows a true regular network after *Smith et al.* [1986], in which a gauge is equidistant from each of its nearest neighbors and thus forms a triangular lattice network. The coefficient of skewness for the overall distribution of intergauge distances is small ($\gamma_d = 0.22$). In this case, the clustering factor is undefined because of the singular value of nearest-neighbor distances ($d_{nn} = 1.0$) for all gauges in the network. The geometry of our 85-gauge WGEW network is examined in Figure 5b, where we find that the overall coefficient of skewness for the distribution of intergauge distance is small ($\gamma_d = 0.68$) and that clustering of gauges is even smaller ($CF = -0.06$).

[25] For comparison, two possible subset networks for the WGEW are shown in Figure 6. A network with $N = 42$ gauges and a $CF < 0$ is shown in Figure 6a, where large nearest-neighbor distances dominate the distribution. This is indicative of a sparse network that may still seem to represent the distribution of precipitation well over the entire WGEW, but at a lower resolution than provided by the complete gauge network. In this case, we suggest that gauge redundancy (a still-ambiguous concept in network analysis) may be reduced, but that the resulting interpolated field will be much smoother than obtained with the complete network.

[26] The coefficient of skewness for the distribution of all intergauge distances in Figure 6a is very near that for a counterpart network subset with $CF > 0$ in Figure 6b. Other statistics of the latter network reflect the small nearest-neighbor distances that dominate the distribution and produce gaps in coverage over the WGEW. While gauge redundancy in the network may not increase above that observed in the complete WGEW network, neither would we find it to be reduced, as for the network with $CF < 0$. We expect increased uncertainty and thus greater errors due to the reduced representation of the complete precipitation field using this network subset. In summary, for networks with $CF < 0$ we expect errors (relative to results for the complete network) due to reduced resolution of the precipitation field, and for networks with $CF > 0$ we expect errors due to reduced areal representation of the precipitation field.

3.2. Spatial Interpolation Methods

[27] This work supports an effort at the selection and implementation of objective analysis methods for application of meteorological observations, especially precipitation, in a distributed LSM framework [*Kumar et al.*, 2006; *Tischler et al.*, 2007]. These methods are investigated with respect to their capability to reproduce certain gauge- and network-provided observations without user interaction or interference. The methods examined here have been selected for their simplicity and relative objectivity in formulation. The first method, interpolation by an inverse-distance-weighted algorithm, has demonstrated efficiency and reliability in consistent operational usage, even in regions of noted orographic influence on precipitation patterns. The second method, interpolation by a multiquadric-biharmonic algorithm, is more sophisticated in formulation than the inverse distance algorithm, and its results have been compared favorably with geostatistics as an objective alternative to that method.

3.2.1. Inverse-Distance-Weighted (IDW) Interpolation

[28] The inverse distance method of spatial interpolation enjoys a long history of usage and reliability, due primarily to its simplicity of formulation and its persistent application in operational settings. This method has been employed for some time in the National Weather Service (NWS) River Forecast System (RFS) [*National Weather Service*, 1999] for the operational estimation of precipitation over much of the United States. The results of inverse distance methods have been compared, often unfavorably, against those of geostatistical methods by several researchers [e.g., *Ball and Luk*, 1998; *Dirks et al.*, 1998].

[29] In the IDW method, the value of the interpolated field p_i at a location (x_i, y_i) is found by

$$p_i = \frac{1}{W_i} \sum_{n=1}^{nn \le N} w_{i,n} p_n, \qquad (4)$$

where p_n is the known value of the field at gauge n. Weights $w_{i,n}$ are given by

$$w_{i,n} = \left[c_x (x_i - x_n)^k + c_y (y_i - y_n)^k + c_z (z_i - z_n)^k \right]^{-1}, \qquad (5)$$

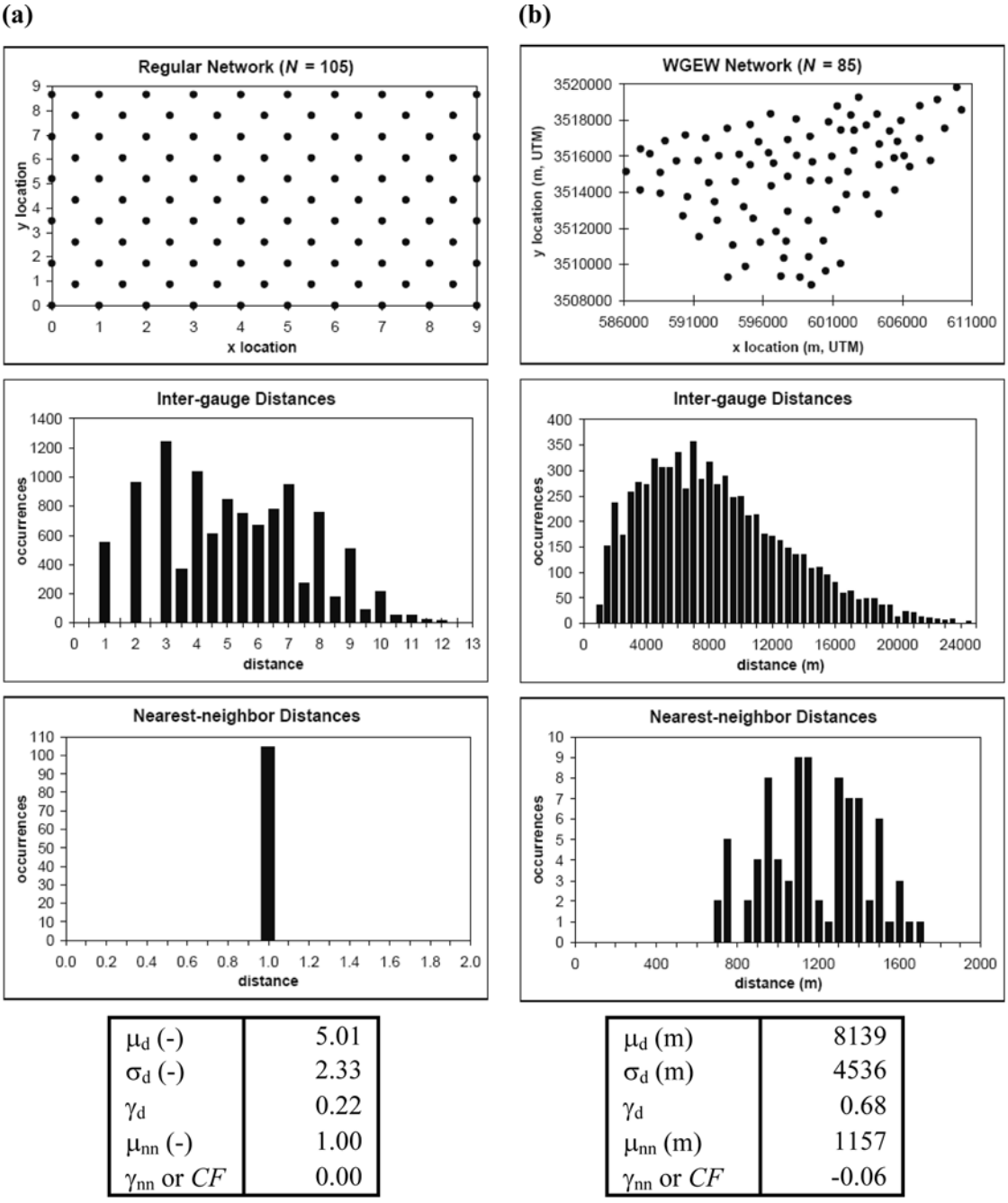

μ_d (-)	5.01
σ_d (-)	2.33
γ_d	0.22
μ_{nn} (-)	1.00
γ_{nn} or *CF*	0.00

μ_d (m)	8139
σ_d (m)	4536
γ_d	0.68
μ_{nn} (m)	1157
γ_{nn} or *CF*	-0.06

Figure 5. Example gauge networks and metric calculations for (a) a regular network ($N = 105$), with a unitless distance measure, and (b) the WGEW network ($N = 85$), with UTM locations in m.

where $\{c_x, c_y, c_z\}$ allow for anisotropic weights, and the normalization factor W_i is found by

$$W_i = \sum_{n=1}^{nn \le N} w_{i,n}. \tag{6}$$

This work will consider only $c_x = c_y = 1$ and $c_z = 0$, indicating horizontally isotropic weighting without explicit topographic influence.

[30] The summations in equations (4) and (6) may be limited in a number of ways, by which a subset of the gauge network is selected according to a "radius of influence" or a specified number of "nearest neighbors" ($nn \le N$) for interpolation to an unknown (or missing) location. It should be noted that, if the limiting value $nn = 1$ is chosen, the mathematics of the IDW method collapse to the selection of the single nearest gauge value, which is the well-known "nearest-neighbor" or *Thiessen* [1911] polygon method for the spatial distribution of precipitation observations. In this work, all available gauges in a network subset are employed in spatial interpolation calculations, such that $1 \le nn < N$.

[31] The order (exponent) k in equation (5) of the IDW algorithm is sometimes at issue in its application. In the NWSRFS and many other examples, $k = 2$ (indicating the inverse-distance-squared method) is widely accepted for

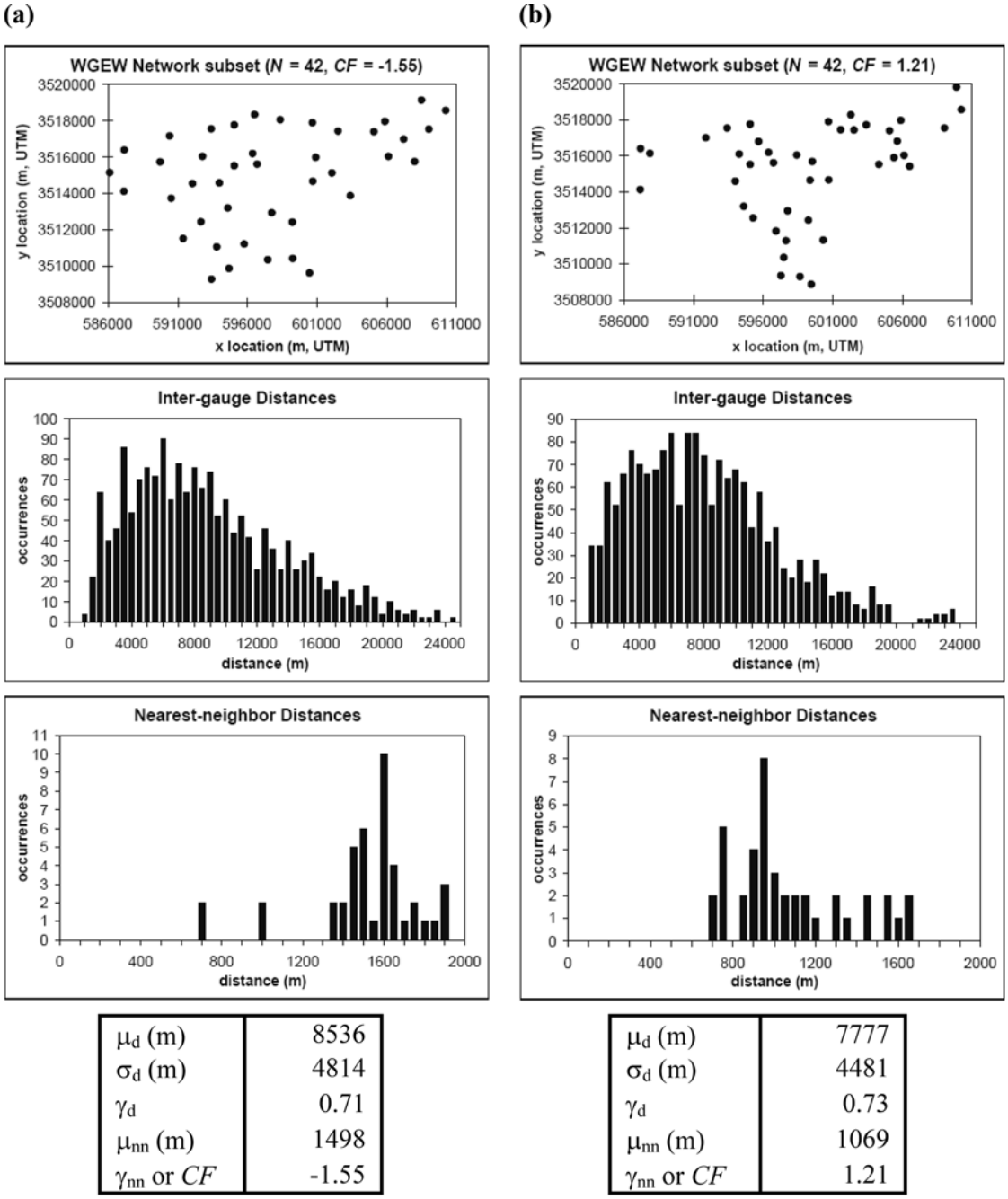

Figure 6. As in Figure 4b, but for WGEW-subset networks with (a) $N = 42$ and $CF < 0$ and (b) $N = 42$ and $CF > 0$.

general use. Several researchers [e.g., *Simanton and Osborn*, 1980; *Tung*, 1983], have experimented with variations in this order, examining its effects on the spatial distribution of information from precipitation observations. The response given by equations (4)–(6) for a linear network of three gauges is illustrated for values of $k = \{1, 2, 3\}$ in Figure 7. Results for these three variations on the IDW algorithm are denoted as IDW-1, IDW-2 and IDW-3, respectively. Evaluation of such experiments requires the reservation of one or more stations in the available network for the purposes of comparison and validation, a difficult task in regions where the gauge coverage is already sparse. In areas of dense gauge coverage, as for the WGEW, this approach becomes more viable and appropriate.

[32] Finally, a computationally attractive feature of the IDW method of spatial interpolation is its capability for precalculation during a numerical simulation, such that time is saved at each interval of the simulation for which new precipitation (or other) input is available. However, this capability relies implicitly on stationarity of the gauge network. These features and capabilities will be important in comparison with the multiquadric-biharmonic interpolation method, described below.

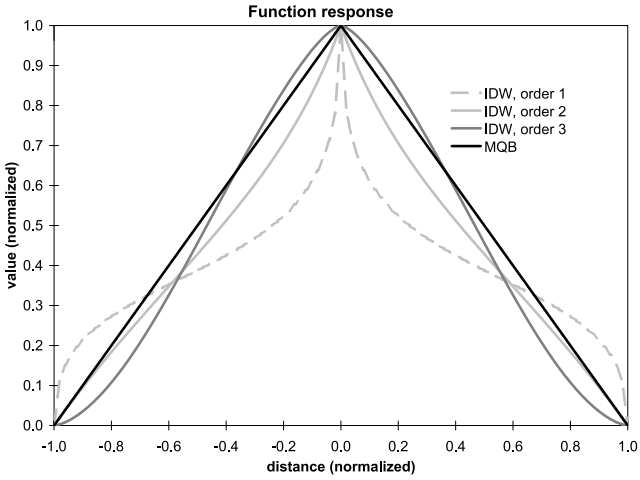

Figure 7. Normalized functional response of interpolation methods for a linear network of three gauges.

3.2.2. Multiquadric-Biharmonic (MQB) Interpolation

[33] Recent exploration and use of the multiquadric-biharmonic (MQB) method for spatial interpolation can be attributed primarily to an extensive review of related work by *Hardy* [1990], the originator of the method. Prior to that time, the MQB method was included in a qualitative comparison of numerous interpolation functions by *Franke* [1982] and in a specific, quantitative comparison with geostatistical methods by *Supachai* [1988]. The latter study found that the MQB method compared favorably with a more subjective geostatistical analysis performed over the same region. The MQB method has since been employed in analyses of precipitation fields on regional [*Nuss and Titley*, 1994] and watershed scales [*Syed*, 1994; *Syed et al.*, 2003]. The work of Syed included comparisons with geostatistical analyses of precipitation patterns over the WGEW during the Monsoon'90 experiment that are directly relevant to the results and discussion presented here.

[34] In the MQB method, the value of the interpolated field q_i at a location (x_i, y_i) is found by

$$q_i = \sum_{n=1}^{N} a_n b_{i,n}, \tag{7}$$

for which the coefficients a_n are determined below and the weights $b_{i,n}$ are given by

$$b_{i,n} = \left[c_x(x_i - x_n)^2 + c_y(y_i - y_n)^2 + c_z(z_i - z_n)^2 + R^2\right]^{1/2}, \tag{8}$$

where the three-dimensional weight is indicated for generality, but again we consider only horizontally isotropic weights with $c_x = c_y = 1$ and $c_z = 0$. The parameter R allows for the fit of a continuously differentiable hyperbolic surface to the given data set [*Hardy*, 1990]; where $R = 0$ is specified, the data set is fitted with conic surfaces that are discontinuous at the given locations. This is illustrated with the response in Figure 7 given by equations (7)–(8) for a linear network of gauges. A detailed analysis of optimal values for the R parameter has been presented by *Carlson and Foley* [1991]. Because the selection of values for R remains nontrivial in practice [e.g., *Franke et al.* 1994], and would change with the gauge network configuration (numbers and locations of gauges), for ease of application we have elected to specify $R = 0$ in this work.

[35] Following the MQB formulations presented by *Hardy* [1990] and *Saunderson* [1992], the coefficients a_n are found by considering that q_j is the known value of the field at gauge j,

$$q_j = \sum_{n=1}^{N} a_n b_{j,n}, \tag{9}$$

or, in matrix notation for the given network,

$$\mathbf{Q}_\mathrm{j} = \mathbf{B}_\mathrm{j,n}\mathbf{A}_\mathrm{n}, \tag{10}$$

for which the terms are given by

$$\mathbf{Q}_\mathrm{j} = \begin{bmatrix} q_1 \\ q_2 \\ \vdots \\ q_N \end{bmatrix}, \mathbf{B}_\mathrm{j,n} = \begin{bmatrix} 0 & b_{1,2} & \cdots & b_{1,N} \\ b_{2,1} & 0 & \cdots & b_{2,N} \\ \vdots & \vdots & \ddots & \vdots \\ b_{N,1} & b_{N,2} & \cdots & 0 \end{bmatrix}, \text{and } \mathbf{A}_\mathrm{n} = \begin{bmatrix} a_1 \\ a_2 \\ \vdots \\ a_N \end{bmatrix}. \tag{11}$$

By premultiplication, the solution for the coefficients $\mathbf{A}_\mathrm{n}$ is obtained as

$$\mathbf{A}_\mathrm{n} = \mathbf{B}_\mathrm{j,n}^{-1}\mathbf{Q}_\mathrm{j}, \tag{12}$$

where the matrix inverse may be found by a preferred algorithm, such as the Gauss-Jordan (employed here) or the least squares methods of inversion. Then, at each time for which spatial interpolation is to be performed, the calculation follows equations (7) and (12) as

$$\mathbf{Q}_\mathrm{i} = \mathbf{B}_\mathrm{i,n}\ \mathbf{A}_\mathrm{n} = \mathbf{B}_\mathrm{i,n}\mathbf{B}_\mathrm{j,n}^{-1}\mathbf{Q}_\mathrm{j}, \tag{13}$$

for which all $b_{i,n}$ and $b_{j,n}$ result from the chosen form of equation (8). It is noted explicitly here that the values in $\mathbf{Q}_\mathrm{j}$ depend on the time series of observations at each gauge location. However, in the context of numerical simulation, the weights for the known gauge locations in $\mathbf{B}_\mathrm{j,n}$ (if stationary) and the inversion and multiplication of that matrix with the simulation domain locations in $\mathbf{B}_\mathrm{i,n}$ may be precalculated, saving computation time in that step of the interpolation process.

3.3. Ensemble Methodology

[36] We evaluate interpolated precipitation amounts at selected points against the recorded precipitation at those locations, essentially in an attempt at reproduction of the "truth" for locations of missing gauge values. The statistics considered here are standard and common representations of comparison error. These statistics include the bias (primarily as an indicator of sampling-related error in ensemble aggregation results), the mean absolute error (MAE), and the root-mean-square error (RMSE).

[37] Of various procedures available for comparisons between subset-based fields $F(x, y, s)$ and the master set–based $F(x, y, S)$, we employ the well-known data denial or

"jackknife" method [*Cressie*, 1993] that relies on the simple removal of source locations for each realization of a subset $F(x, y, s)$. For each subset, the field values at "missing" locations may be found by the described interpolation methods using only those gauges in the subset, and the resulting values may then be compared with those in the full set, $F(x, y, S)$. In these experiments, a random nonrepeating ensemble of gauge subsets was selected for each value of $1 \leq n \leq 84$ for individual comparison with the full set of gauges ($N = 85$). This methodology is somewhat analogous to the Monte Carlo method employed by *Krajewski et al.* [1991]. The results of these comparisons were then aggregated and analyzed for the statistics reported below.

[38] The number of required, randomly selected subsets N_S for statistical significance of the aggregated ensemble results may be found, after *Cressie* [1993], by

$$N_S = \frac{t(c)}{p}, \tag{14}$$

where the precision of the estimate is indicated by p and the function t represents Student's t distribution on the basis of the desired confidence c in the estimate. However, with expected errors of 0.25 mm (0.01 inches, the measurement resolution of most precipitation gauges in the United States) at a confidence level of 99.9%, only 14 subsets are required for evaluation, and we have found that this small ensemble size results in potentially large biases in the aggregated results. Even at an expected error of 0.10 mm, at the same level of confidence, the calculated 33-subset ensembles still allow some undesirable bias at low network densities in the aggregated results. We have thus elected here to evaluate ensembles with 66 members (i.e., randomly selected gauge network subsets) in the space of $1 \leq n \leq 84$, with expected errors of 0.05 mm at a confidence level of 99.9%. These selections are applied to produce randomly selected, nonrepeating subsets of the complete gauge network for analysis according to the jackknife method.

4. Results and Discussion

[39] Aggregated error statistics of the randomly selected ensembles, as described above, are analyzed with respect to both gauge network density, represented by the number of gauges N in the network, and the calculated clustering factor CF for the ensemble member. The impacts of these results on the selection and optimization of an interpolation method according to event morphology are also discussed.

4.1. Error as a Function of Network Density

[40] Graphical results showing the ensemble mean MAE and RMSE with respect to the number of gauges N in the subset network, evaluated against the full network, are shown for event 1 in Figure 8a. It is clear that the IDW-1 method produces far inferior results, that the IDW-2 method produces slightly larger errors than its higher-order counterpart, and that results of the IDW-3 and MQB methods are nearly indistinguishable over much of the set space.

[41] Similar results are found for event 2, as shown in Figure 8b. However, it is clear that the MQB method performs better than all orders of the IDW method in this case. The overall magnitudes of MAE and RMSE increase with the spatial CV of the events and are consistent with the analysis of convective and stratiform character for each event as discussed above.

[42] The bias results for each event are not shown, but were different for each of the interpolation methods and are described here. For event 1, bias results were found to range up to 2.5 mm, which is 6.4% of the mean and only 3.0% of the maximum event precipitation as listed in Table 1. Interpolation biases were found to remain above 1% of the mean event precipitation only for low network subset densities, up to approximately one third of the complete WGEW gauge network ($n \leq 28$). For event 2, bias results ranged up to 4.5 mm, which is 34.1% of the mean but only 6.6% of the maximum event precipitation. For this more convective case, interpolation biases were found to remain above 10% of the mean event precipitation for network subset densities up to approximately one sixth of the complete WGEW gauge network ($n \leq 13$) and above 1% for network subset densities up to approximately three quarters of the complete network ($n \leq 66$). Overall, these results suggest an exponential decrease in interpolation bias with network density, though this factor may be explained by the consideration of still too few ensemble members at those network densities in the jackknife method employed here.

[43] It is evident in these results that event 2, of more distinctly convective morphology, produces greater values of MAE and RMSE than the mixed morphology of event 1. As expected, it is more difficult to describe accurately the spatial distribution of precipitation in a convective event with a limited or partial network than with the complete network, regardless of the interpolation method selected. This conclusion presents significant implications for other locations with less dense gauge networks. Specifically, the accuracy to be expected from an interpolator operation is limited inherently by the spatial resolution provided by the gauge network. We suggest that the interpolation order, resulting errors, the gauge network density (or a proxy measure, such as the mean spacing of nearest neighbors), and the characteristic spatial scale of the precipitation event must all be considered together in such analyses. For isolated or strongly convective events, such as event 2 examined here, large errors must be expected where the surface gauge network remains inadequate for the observation and spatial representation of the event dynamics, for which no method of interpolation based purely on mathematics can compensate. In such a case, ancillary information (e.g., topography, where orographic influences are suspected) and dynamical models represent more physically based, and potentially more accurate, approaches to the problem of event analysis.

4.2. Error as a Function of Network Geometry

[44] Graphical results showing the individual gauge network subset values of MAE and RMSE with respect to the calculated subset clustering factor CF are shown for event 1 in Figure 9a. Results for the IDW-1 method are not shown, but more than 5,400 ensemble member results for each of the other interpolation methods (IDW-2, IDW-3 and MQB) were analyzed in the demonstration of these error metrics. A close-up view of the range in results for $-3 < CF < 3$ is shown here, though the complete set of analysis results

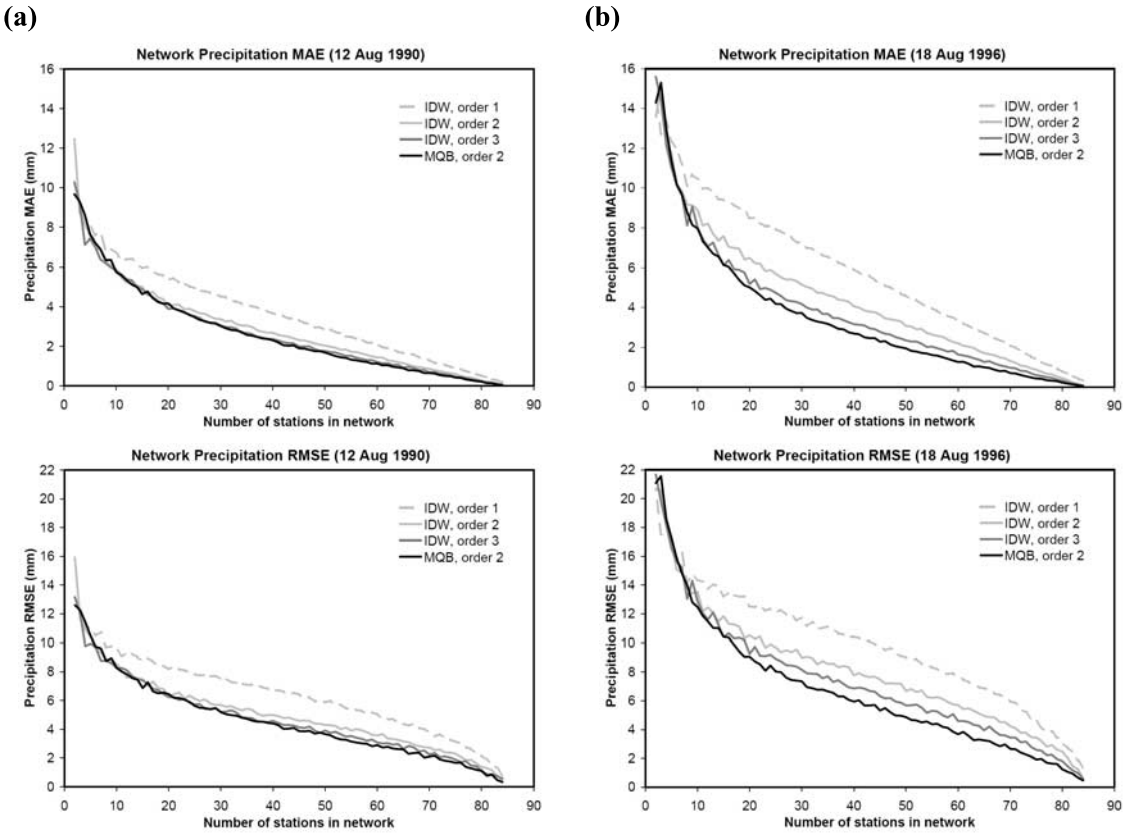

Figure 8. Plots of (top) *MAE*(*N*) and (bottom) *RMSE*(*N*) for (a) event 1 on 12 August 1990 and (b) event 2 on 18 August 1996.

spanned the range $-13 < CF < 75$ for this event. Within the range shown, results for nearly 54% of the complete set are represented. It is evident that the calculated errors are generally smaller, and depend less on the selection of interpolation method, for $CF < 0$. For networks with $CF > 0$, greater differences between the results of the various interpolation methods are shown.

[45] The corresponding error results for event 2 are shown in Figure 9b. In this case, the range $-3 < CF < 3$ shown there represents more than 79% of the results for the complete set of interpolation experiments, which spanned the range $-16 < CF < 74$ for this event. Again, the calculated errors are generally smaller and less dependent on the selection of interpolation method for $CF < 0$, though larger differences between the interpolation methods are evident for this event than for event 1. For networks with $CF > 0$, greater differences in results of the various interpolation methods are again apparent.

[46] Overall, it is concluded that the MQB interpolation method performs best but, like the IDW methods, remains subject to significant errors when clustering of the gauge network prevents adequate spatial coverage and thus representation of the observed storm event. In all cases, it is shown that better results are obtained for gauge networks that are less clustered in geometry and can better represent the overall spatial coverage and observed resolution of the convective events. As discussed above, for networks with $CF < 0$ the calculated errors remain relatively smaller and are due primarily to reduced resolution of the precipitation field, while for networks with $CF > 0$, calculated errors are relatively larger and are more likely due to missed features in the precipitation field because of reduced areal representation.

4.3. Discrimination and Interpolation According to Event Morphology

4.3.1. Discrimination Methodology

[47] The discrimination of convective and stratiform events was not solely based on the calculated spatial *CV*, but primarily on the analysis of breakpoint and hourly precipitation rates during the event and additional knowledge of the event environment. It would certainly be advantageous to develop a method of event discrimination based on the calculated spatial statistics of the events, e.g., spatial minimum and maximum precipitation rates, spatially distributed total event precipitation, and spatial moments including variance and *CV* as listed in Table 1. However, in both the convective and mixed or stratiform events examined here it was found that the MQB interpolation method generally outperformed the IDW interpolation methods, leaving little additional information to be provided to the interpolation selection or method formulation by the discrimination according to event morphology.

4.3.2. Interpolator Selection and Optimization

[48] For holistic evaluation of the precipitation field over a limited gauge network, the MQB interpolation method seems to provide better error characteristics than the IDW methods examined here. The MQB method is followed

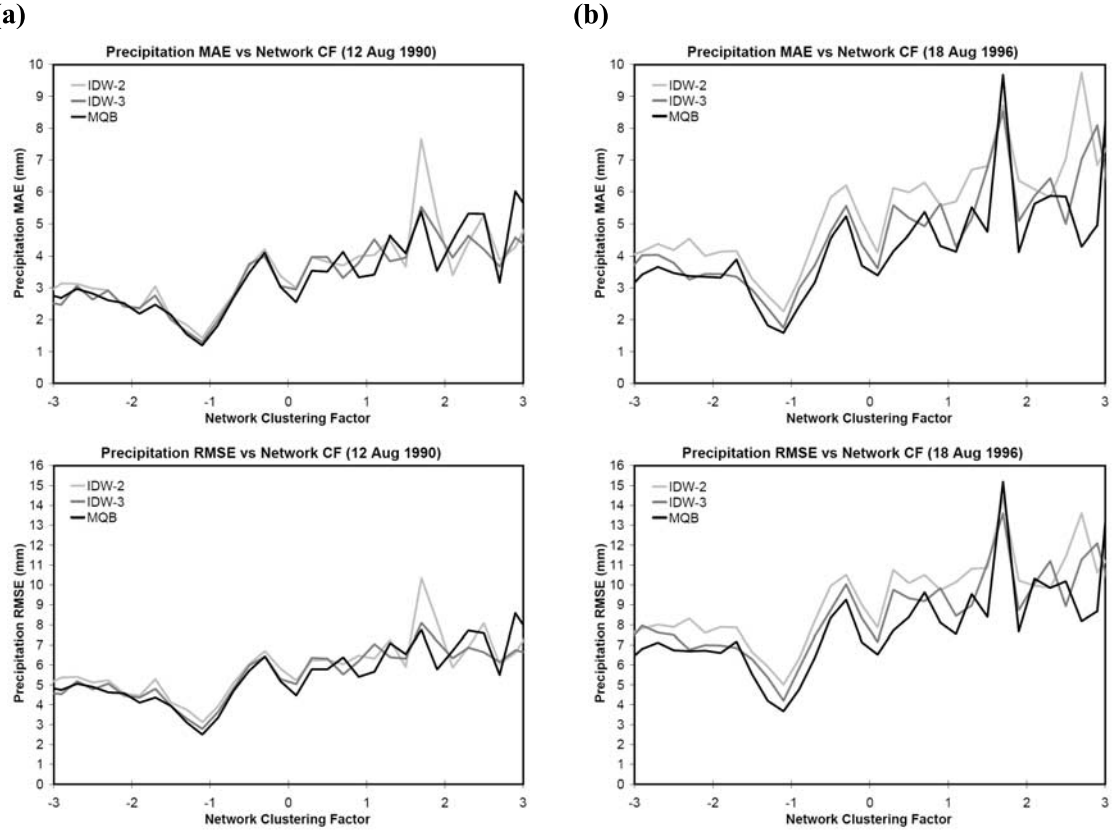

Figure 9. Plots of (top) *MAE*(*CF*) and (bottom) *RMSE*(*CF*) for (a) event 1 on 12 August 1990 and (b) event 2 on 18 August 1996.

closely in accuracy by the IDW-3 method, which provides nearly equivalent results for stratiform events. Greater differences between the interpolation methods should be expected for events of more convective character, and especially for clustered networks ($CF > 0$). Interpolation experiments with small, idealized gauge networks have suggested that the MQB method is insensitive to the impacts of clustering on interpolation results, while the IDW method may erroneously weight duplicate information equally in gauge clusters (G. Woodard, personal communication, 2007). This result lends justification to the use of MQB results as a baseline, and suggests that it may be possible to incorporate information on gauge clusters into the IDW formulation, bringing its results closer to those of the MQB method. The IDW-2 method, a common and accepted choice in operational settings, is clearly not as accurate as its higher-order counterpart in convective conditions. These results extend the work of *Simanton and Osborn* [1980], who considered only simple correlation in their assessment of IDW interpolation accuracy at various orders.

[49] The computational burden of the interpolation method increases with the number of gauges in the observation network. This is especially the case for the MQB method because of the matrix inversion and multiplication operations required. It is likely a better approach to employ the IDW-3 method, which provides comparable results for mixed and stratiform events, when computational constraints are at issue. There is no obvious difference in computational burden between IDW-2 and IDW-3 methods.

[50] We may also consider the application of interpolation methods in a targeted "window" approach, where the MQB method could be applied to isolated convective events and the IDW-3 method could be applied to larger mixed or stratiform events and over larger areas. It is likely easier to apply the IDW-3 method in a "moving window" approach on the basis of a limited number of nearest neighbors, or with a fixed radius of influence, because of the formulation mathematics involved. The MQB method requires consideration and operation on the entire network in the observation window, likely lending difficulty to the application of that method over larger areas where the influence of distant gauge observations on interpolation at a particular location is expected to remain small or negligible. In such a case, the IDW methods are inherently better suited to the interpolation of the precipitation field.

5. Summary and Conclusions

[51] Discrimination of event morphology according to spatial *CV*, and its potential correlation with the selection and effectiveness of applied interpolation methods, has been examined here. The clustering factor *CF* was formulated from the coefficient of skewness for the distribution of nearest-neighbor distances in the gauge network, as an indicator of clustering in the observing network. A simple jackknife analysis demonstrated the performance of MQB and IDW interpolation methods at various orders, though it was found that a greater number of ensemble members may still be required for the reduction of residual bias in the

results and for more thorough sampling throughout the range of *CF*. Overall, the MQB and IDW-3 methods produce superior error statistics in events of mixed or stratiform morphology and for networks with $CF < 0$. In convective events, the MQB method produced clearly more accurate interpolation results, and for clustered networks ($CF > 0$) was more accurate than the IDW methods by a small margin. In all cases, the IDW-2 method, a common choice, is not as accurate as the MQB and IDW-3 methods.

[52] It is difficult to determine how the *CF* could best be incorporated into the mathematical formulation of interpolation functions in order to reduce the influence of redundant gauges, but some precedent is available [e.g., *Habib et al.*, 2001; *Daly et al.*, 2002; *Ahrens*, 2006]. The distributions of error with respect to network geometry (specifically, clustering) may be useful for a priori estimates of expected error for a reduced network and for particular precipitation event morphology, with proper consideration given to the method and order of interpolation selected. As mentioned above, however, such mathematical considerations may remain unnecessary in use of the MQB method for spatial interpolation. This aspect of MQB utility, especially in studies of networks with large numbers of gauge locations and thus considerable computational burden, remains an issue for further investigation.

[53] It is recognized that the results of the analyses presented here may remain specific to the region, time period, and weather and climate regimes studied. As described above, the rainfall records examined in this work occurred in a semiarid region of moderate orographic influence and during a portion of the boreal summer season under the synoptic influence of the NAM system. For application to other locations, time periods, and weather and climate regimes, it is intended that the described methodology will remain robust, though the results of an individual application may differ significantly from those discussed here.

[54] **Acknowledgments.** The authors gratefully acknowledge the support and assistance of M. Susan Moran and Carl Unkrich (USDA-ARS), Michael Tischler (USACE-TEC), Joseph Santanello (UMD-ESSIC and NASA-GSFC), David Mocko and Scott Rheingrover (SAIC and NASA-GSFC), Gary Woodard (UA-SAHRA), and numerous reviewers. This research was supported by the U.S. Army Corps of Engineers and the USDA Agricultural Research Service, with contributed effort of additional USDA-ARS and NASA-GSFC employees.

References

Adams, D. K., and A. C. Comrie (1997), The North American monsoon, *Bull. Am. Meteorol. Soc.*, *78*, 2197–2213.

Ahrens, B. (2006), Distance in spatial interpolation of daily rain gauge data, *Hydrol. Earth Syst. Sci.*, *10*, 197–208.

Ball, J. E., and K. C. Luk (1998), Modeling spatial variability of rainfall over a catchment, *J. Hydrol. Eng.*, *3*, 122–130.

Blöschl, G., and M. Sivapalan (1995), Scale issues in hydrological modelling—A review, *Hydrol. Processes*, *9*, 251–290.

Bradley, A. A., C. Peters-Lidard, B. R. Nelson, J. A. Smith, and C. B. Young (2002), Raingage network design using NEXRAD precipitation estimates, *J. Am. Water Resour. Assoc.*, *38*, 1393–1407.

Bras, R. F., and I. Rodríguez-lturbe (1976), Network design for the estimation of areal mean rainfall events, *Water Resour. Res.*, *12*, 1185–1195.

Briggs, P. R., and J. G. Cogley (1996), Topographic bias in mesoscale precipitation networks, *J. Clim.*, *9*, 205–218.

Carlson, R. E., and T. A. Foley (1991), The parameter R^2 in multiquadric interpolation, *Comput. Math. Appl.*, *21*, 29–42.

Carpenter, T. M., and K. P. Georgakakos (2004), Impacts of parametric and radar rainfall uncertainty on the ensemble streamflow simulations of a distributed hydrologic model, *J. Hydrol.*, *298*, 202–221.

Chaubey, I., C. T. Haan, J. M. Salisbury, and S. Grunwald (1999), Quantifying model output uncertainty due to spatial variability of rainfall, *J. Am. Water Resour. Assoc.*, *35*, 1113–1123.

Cosgrove, B. A., et al. (2003), Real-time and retrospective forcing in the North American Land Data Assimilation System (NLDAS) project, *J. Geophys. Res.*, *108*(D22), 8842, doi:10.1029/2002JD003118.

Cressie, N. A. C. (1993), *Statistics for Spatial Data*, John Wiley, New York.

Daly, C., W. P. Gibson, G. H. Taylor, G. L. Johnson, and P. Pasteris (2002), A knowledge-based approach to the statistical mapping of climate, *Clim. Res.*, *22*, 99–113.

Dirks, K. N., J. E. Hay, C. D. Stow, and D. Harris (1998), High-resolution studies of rainfall on Norfolk Island, part II: Interpolation of rainfall data, *J. Hydrol.*, *208*, 187–193.

Eagleson, P. S. (1967), Optimum density of rainfall networks, *Water Resour. Res.*, *3*, 1021–1033.

Faurès, J.-M., D. C. Goodrich, D. A. Woolhiser, and S. Sorooshian (1995), Impact of small-scale spatial rainfall variability on runoff modeling, *J. Hydrol.*, *173*, 309–326.

Franke, R. (1982), Scattered data interpolation: Tests of some methods, *Math. Comput.*, *38*, 181–200.

Franke, R., H. Hagen, and G. M. Nielson (1994), Least squares surface approximation to scattered data using multiquadratic functions, *Adv. Comput. Math.*, *2*, 81–99.

Germann, U., and J. Joss (2000), Spatial continuity of Alpine precipitation, *Phys. Chem. Earth B*, *25*, 903–908.

Germann, U., and J. Joss (2001), Variograms of radar reflectivity to describe the spatial continuity of Alpine precipitation, *J. Appl. Meteorol.*, *40*, 1042–1059.

Goodrich, D. C., L. J. Lane, R. M. Shillito, S. N. Miller, K. H. Syed, and D. A. Woolhiser (1997), Linearity of basin response as a function of scale in a semiarid watershed, *Water Resour. Res.*, *33*, 2951–2965.

Goodrich, D. C., T. O. Keefer, C. L. Unkrich, M. H. Nichols, H. B. Osborn, J. J. Stone, and J. R. Smith (2008), Long-term precipitation database, Walnut Gulch Experimental Watershed, Arizona, United States, *Water Resour. Res.*, doi:10.1029/2006WR005782, in press.

Habib, E., W. F. Krajewski, and G. J. Ciach (2001), Estimation of rainfall interstation correlation, *J. Hydrometeorol.*, *2*, 621–629.

Hardy, R. L. (1990), Theory and applications of the multiquadric-biharmonic method, *Comput. Math. Appl.*, *19*, 163–208.

Higgins, R. W., Y. Yao, and X. L. Wang (1997), Influence of the North American monsoon system on the U.S. summer precipitation regime, *J. Clim.*, *10*, 2600–2622.

Higgins, W., et al. (2006), The NAME 2004 field campaign and modeling strategy, *Bull. Am. Meteorol. Soc.*, *87*, 79–94.

Houze, R. A. Jr. (2004), Mesoscale convective systems, *Rev. Geophys.*, *42*, RG4003, doi:10.1029/2004RG000150.

Humphrey, M. D., J. D. Istok, J. Y. Lee, J. A. Hevesi, and A. L. Flint (1997), A new method for automated dynamic calibration of tipping-bucket rain gauges, *J. Atmos. Oceanic Technol.*, *14*, 1513–1519.

Jackson, T. J., and D. P. Lettenmaier (2004), Soil Moisture Experiments 2004 (SMEX04), *Eos Trans. AGU*, *85*(17), Jt. Assem. Suppl., Abstract H11B-03.

Krajewski, W. F., V. Lakshmi, K. P. Georgakakos, and S. C. Jain (1991), A Monte Carlo study of rainfall sampling effect on a distributed catchment model, *Water Resour. Res.*, *27*, 119–128.

Kumar, S. V., et al. (2006), Land information system: An interoperable framework for high resolution land surface modeling, *Environ. Modell. Software*, *21*, 1402–1415.

Kustas, W. P., et al. (1991), An interdisciplinary study of the energy and water fluxes in the atmosphere-biosphere system over semiarid rangelands: Description and some preliminary results, *Bull. Am. Meteorol. Soc.*, *72*, 1683–1706.

Larson, L. W., and E. L. Peck (1974), Accuracy of precipitation measurements for hydrologic modeling, *Water Resour. Res.*, *10*, 857–863.

Maddox, R. A., D. M. McCollum, and K. W. Howard (1995), Large-scale patterns associated with severe summertime thunderstorms over central Arizona, *Weather Forecasting*, *10*, 763–778.

Matalas, N. C., and E. J. Gilroy (1968), Some comments on regionalization in hydrologic studies, *Water Resour. Res.*, *4*, 1361–1369.

McCollum, J. R., and W. F. Krajewski (1998), Uncertainty of monthly rainfall estimates from rain gauges in the Global Precipitation Climatology Project, *Water Resour. Res.*, *34*, 2647–2654.

Morrissey, M. L., J. A. Maliekal, J. S. Greene, and J. Wang (1995), The uncertainty of simple spatial averages using rain gauge networks, *Water Resour. Res.*, *31*, 2011–2017.

National Weather Service (1999), National Weather Service River Forecast System (NWSRFS) user's manual, Off. of Hydrol., Natl. Weather Serv., NOAA, Silver Spring, Md.

Nijssen, B., and D. P. Lettenmaier (2004), Effect of precipitation sampling error on simulated hydrological fluxes and states: Anticipating the Global Precipitation Measurement satellites, *J. Geophys. Res.*, *109*, D02103, doi:10.1029/2003JD003497.

Nuss, W. A., and D. W. Titley (1994), Use of multiquadric interpolation for meteorological objective analysis, *Mon. Weather Rev.*, *122*, 1611–1631.

Nykanen, D. K., E. Foufoula-Georgiou, and W. M. Lapenta (2001), Impact of small-scale rainfall variability on larger-scale spatial organization of land-atmosphere fluxes, *J. Hydrometeorol.*, *2*, 105–121.

Pardo-Igúzquiza, E. (1998), Optimal selection of number and location of rainfall gauges for areal rainfall estimation using geostatistics and simulated annealing, *J. Hydrol.*, *210*, 206–220.

Parker, M. D., and R. H. Johnson (2000), Organizational modes of midlatitude mesoscale convective systems, *Mon. Weather Rev.*, *128*, 3413–3436.

Parker, M. D., and R. H. Johnson (2004), Structures and dynamics of quasi-2D mesoscale convective systems, *J. Atmos. Sci.*, *61*, 545–567.

Raymond, D. J. (1981), Simulation of an air-mass thunderstorm using the 2-scale model, *J. Atmos. Sci.*, *38*, 2014–2020.

Rodríguez-Iturbe, I., and J. M. Mejía (1974), The design of rainfall networks in time and space, *Water Resour. Res.*, *10*, 713–728.

Sansom, J. (1992), Breakpoint representation of rainfall, *J. Appl. Meteorol.*, *31*, 1514–1519.

Saunderson, H. C. (1992), Multiquadric interpolation of fluid speeds in a natural river channel, *Comput. Math. Appl.*, *24*, 187–193.

Sevruk, B. (1996), Adjustment of tipping-bucket precipitation gauge measurements, *Atmos. Res.*, *42*, 237–246.

Simanton, J. R., and H. B. Osborn (1980), Reciprocal-distance estimate of point rainfall, *J. Hydraul. Eng.*, *106*, 1242–1246.

Skøien, J. O., G. Blöschl, and A. W. Western (2003), Characteristic space scales and timescales in hydrology, *Water Resour. Res.*, *39*(10), 1304, doi:10.1029/2002WR001736.

Smith, D. R., M. E. Pumphry, and J. T. Snow (1986), A comparison of errors in objectively analyzed fields for uniform and nonuniform station distributions, *J. Atmos. Oceanic Technol.*, *3*, 84–97.

Steiner, M., and J. A. Smith (1998), Convective versus stratiform rainfall: An ice-microphysical and kinematic conceptual model, *Atmos. Res.*, *48*, 317–326.

Supachai, S. (1988), Comparative studies of kriging, multiquadric-biharmonic, and other methods for solving mineral resource problems. Ph.D. dissertation, Dep. of Earth Sci., Iowa State Univ. of Sci. and Technol., Ames.

Syed, K. H. (1994), Spatial storm characteristics and basin response, M. S. thesis, Dep. of Hydrol. and Water Resour., Univ. of Ariz., Tucson.

Syed, K. H., D. C. Goodrich, D. E. Myers, and S. Sorooshian (2003), Spatial characteristics of thunderstorm rainfall fields and their relation to runoff, *J. Hydrol.*, *271*, 1–21.

Taylor, C. M., R. J. Harding, A. J. Thorpe, and P. Bessemoulin (1997), A mesoscale simulation of land surface heterogeneity from HAPEX-Sahel, *J. Hydrol.*, *189*, 1040–1066.

Thiessen, A. H. (1911), Precipitation averages for large areas, *Mon. Weather Rev.*, *39*, 1082–1084.

Tischler, M., M. Garcia, C. Peters-Lidard, M. S. Moran, S. Miller, D. Thoma, S. Kumar, and J. Geiger (2007), A GIS framework for surface-layer soil moisture estimation combining satellite radar measurements and land surface modeling with soil physical property estimation, *Environ. Modell. Software*, *22*, 891–898.

Tsintikidis, D., K. P. Georgakakos, J. A. Sperfslage, D. E. Smith, and T. M. Carpenter (2002), Precipitation uncertainty and raingauge network design within Folsom Lake watershed, *J. Hydrol. Eng.*, *7*, 175–184.

Tung, Y.-K. (1983), Point rainfall estimation for a mountainous region, *J. Hydraul. Eng.*, *109*, 1386–1393.

Upton, G. J. G., and A. R. Rahimi (2003), On-line detection of errors in tipping-bucket raingauges, *J. Hydrol.*, *278*, 197–212.

Woods, R., and M. Sivapalan (1999), A synthesis of space-time variability in storm response: Rainfall, runoff generation, and routing, *Water Resour. Res.*, *35*, 2469–2485.

M. Garcia and C. D. Peters-Lidard, Hydrological Sciences Branch, NASA-GSFC, Code 614.3, Greenbelt, MD 20771, USA. (matthew.garcia@nasa.gov)

D. C. Goodrich, Southwest Watershed Research Center, ARS, USDA, 2000 E. Allen Road, Tucson, AZ 85719, USA.